

Highly water-stable rare ternary Ag–Au–Se nanocomposites as long blood circulation time X-ray computed tomography contrast agents†

Carlos Caro,^{a,b} Mariona Dalmases,^{c,d} Albert Figuerola,^{c,d} María Luisa García-Martín,^{a,*}
Manuel Pernia Leal^{a,b,*}

^aBIONAND, Andalusian Centre for Nanomedicine and Biotechnology (Junta de Andalucía-Universidad de Málaga), Málaga, Spain

^bDepartamento de Química Orgánica y Farmacéutica, Universidad de Sevilla, 41012 Seville, Spain

^cInstitut de Nanociència i Nanotecnologia (IN2UB), Universitat de Barcelona, Martí i Franquès 1-11, 08028 Barcelona, Spain

^dDepartament de Química Inorgànica i Orgànica, Secció de Química Inorgànica, Universitat de Barcelona, Martí i Franquès 1-11, 08028 Barcelona, Spain

* email: mpernia@us.es; mlgarcia@bionand.es

Index

1. DLS stability
2. UV-Vis spectroscopy
3. XRD
4. Cell morphology studies
5. Biodistribution
 - a) ICP of the major organs
 - b) CT of the heart
6. Side effects
 - a) Histology of mouse after MNP injection

b) Weight control of the animal

1. Stability DLS

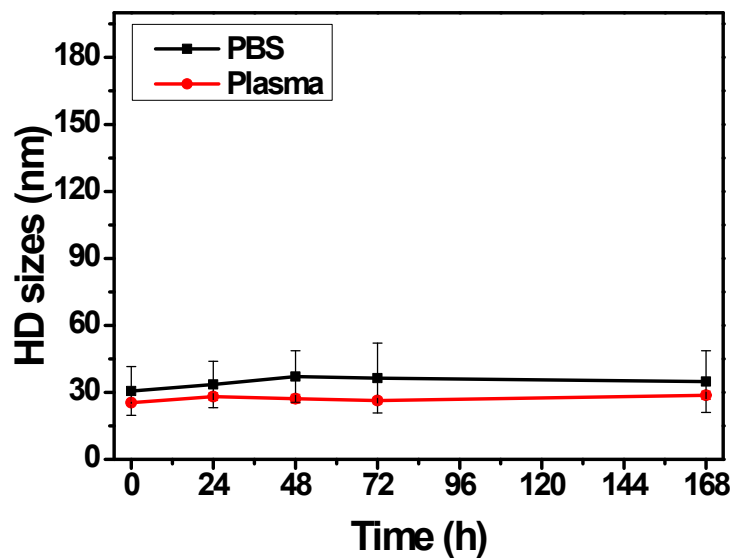


Figure S1. Colloidal stability of PEGylated Ag_3AuSe_2 NPs vs. time in PBS buffer (black curve) and plasma (red curve).

2. UV-Vis spectroscopy

One of the main properties of the silver/gold nanoparticles is the Surface Plasmon Resonance (SPR), which could be defined as a quantized collective oscillation of conduction electron confined in a metal/dielectric boundary that strongly interacts with electromagnetic field,¹ promoting for example strong absorption band in the visible region of electromagnetic spectrum.

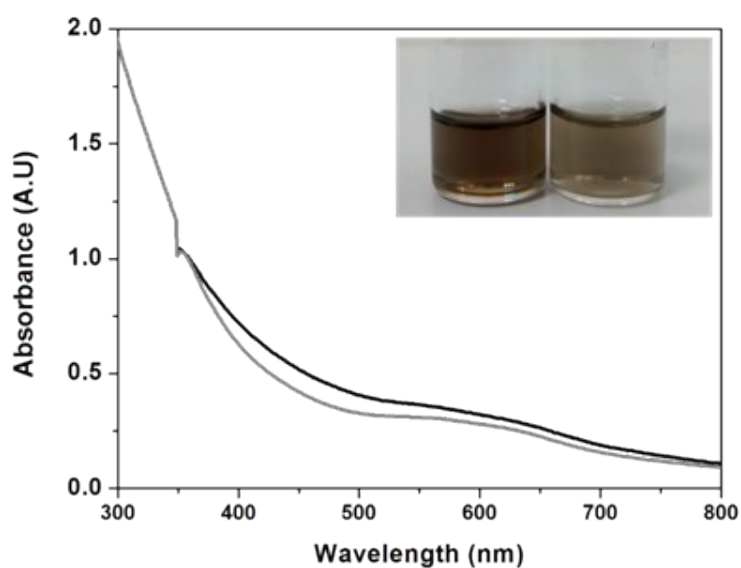


Figure S2. UV-Vis spectrum of the DHLA acid-PEGn-OH ternary NPs and ternary NPs before the ligand exchange process (grey) showing the plasmonic absorption band in the range between 500-700 nm (black), and a picture of the NPs suspension before (left) and after (right) functionalization (inset).

3. XRD

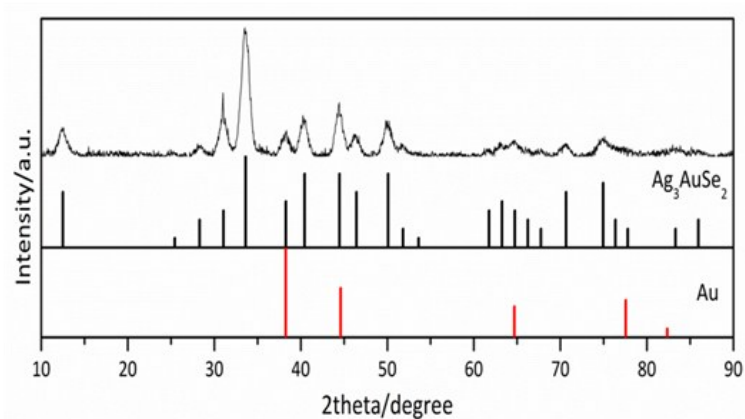


Figure S3. XRD spectrum of the ternary NPs.

4. Cell morphology studies

The C6 cells were plated at a density of 1×10^4 cells/well in a 96-well plate at 37°C in 5% CO₂ atmosphere (200 µL per well, number of repetitions = 5). After 24 h of culture, the medium in the wells was replaced with fresh medium containing the PEGylated ternary NPs in varying concentrations from 0.5 µg/mL to 500 µg/mL. Similarly to the cytotoxicity assays, after 24 h, the Triton X-100 was added to the positive control wells. After 15 min, all the wells were stained with DAPI (4',6-Diamidino-2-phenylindole) (dilution 1:3000) to label nuclei in all cells, although with stronger labeling in live cells, and Propidium Iodine (PI) to only label dead cells (dilution 1:1000). The cell morphology images were acquired using a Perkin Elmer Operetta High Content Imaging System with a 20x LWD 0.45 NA air objective lens. 5 well replicas for each condition were analyzed with 10 random image fields captured per well. For each field, fluorescence images for DAPI and PI, plus a brightfield image were captured. Cell mortality percentages were calculated automatically by Operetta Harmony software, whereby all nuclei (dead and alive) were identified from the DAPI staining and the percentage of dead cells then determined by the number of nuclei also possessing high levels of PI staining.

In agreement with the result shown by the MTT assay, the morphology of the cell remains unaltered till the concentration 250 µg/mL of the PEGylated nanoparticles. Moreover, the analysis of cell mortality also closely matches the MTT experiment.

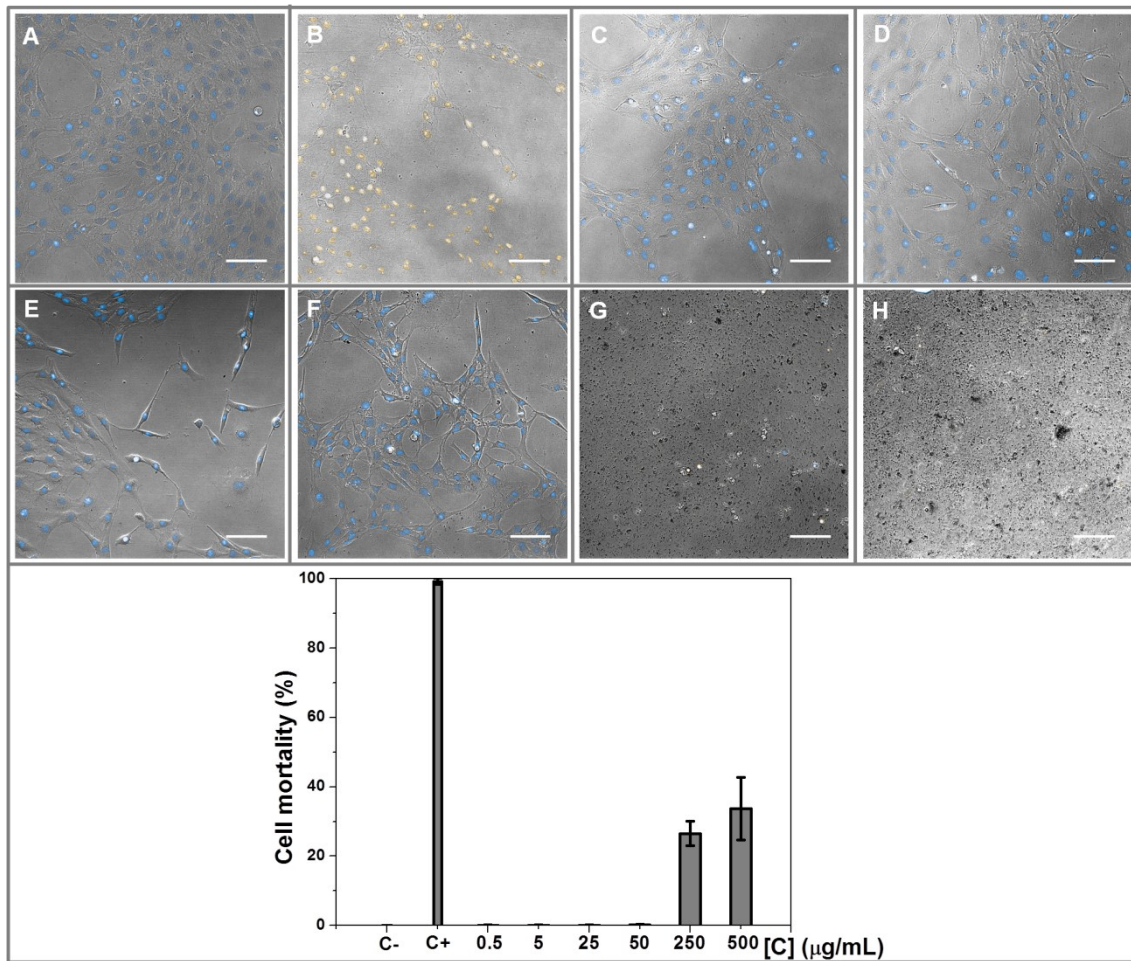


Figure S4. Images of the cultured cell exposed to different concentration of PEGylated nanoparticles: A) Negative control, B) Positive control, C) 0.5 µg/mL, D) 5 µg/mL, E) 25 µg/mL, F) 50 µg/mL, G) 250 µg/mL and H) 500 µg/mL. The images show the merge of brightfield (grey), DAPI (blue) and Propidium Iodine (yellow). In the lower panel a graph of average cell mortality, calculated by automated analysis of DAPI and PI fluorescence images.

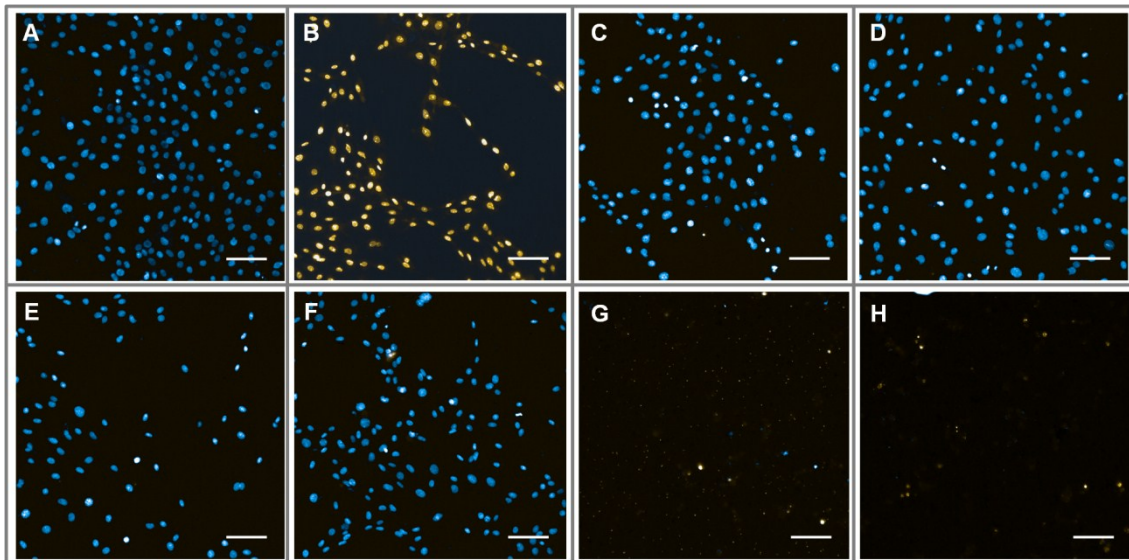


Figure S5. Images of the cultured cell exposed to different concentration of PEGylated nanoparticles: A) Negative control, B) Positive control, C) 0.5 $\mu\text{g/mL}$, D) 5 $\mu\text{g/mL}$, E) 25 $\mu\text{g/mL}$, F) 50 $\mu\text{g/mL}$, G) 250 $\mu\text{g/mL}$ and H) 500 $\mu\text{g/mL}$. The images show the merge of DAPI (blue) and Propidium Iodine (yellow).

5. Biodistribution

a) ICP of major organs

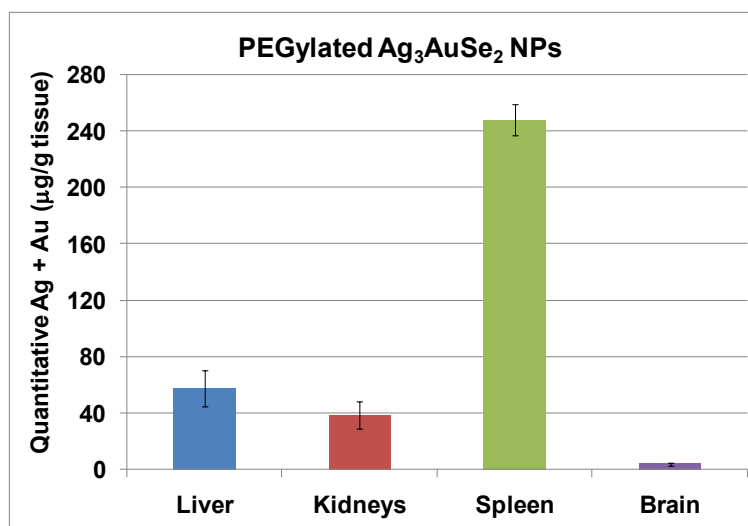


Figure S6. Biodistribution of ternary nanoparticles. Nanoparticles were administered intravenously in balb/c mice (n = 3) and 1 h after injection the amount of Ag and Au was quantified post-mortem in different organs by ICP-MS.

b) CT of the heart.

The time-course of ternary NPs in the heart was followed by quantifying the signal attenuation of CT images acquired at 1, 24, 48 and 72 h. The results showed that ternary NPs were slowly cleared from the bloodstream, remaining at least 24 h post-injection. These results are in good agreement with the CT measurements performed post-mortem in the blood of mice injected with ternary NPs.

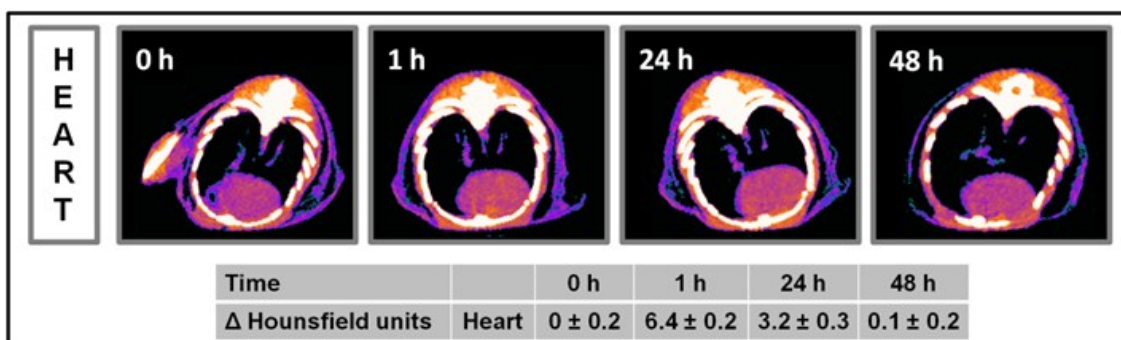


Figure S7. Representative *in vivo* CT images of the heart at different experimental times after the intravenous injection of ternary NPs. Values are Hounsfield units with the intensity scale set to visualize differences between soft tissues (leaving the bones overexposed). The table at the bottom shows the increment in Hounsfield units at different times after the intravenous injection of ternary NPs (n=3).

6. Side effects

A fundamental point in the use of nanoparticles as contrast agents in diagnostic imaging is to evaluate the potential side effects that they could cause in the organism. Thus, to evaluate possible side effects we performed histological analysis of the major organs by

optical microscopy. Also, the animals' weight was monitored daily up to one week after treatment.

a) Histology:

The microscopic evaluation of the histological sections of major organs, stained with haematoxylin-eosin, did not show any sign of tissue damage, as can be seen in Figure S8 (histology of liver and renal cortex) or Figure S9 and Figure S10 (histology of renal medulla and spleen, respectively).

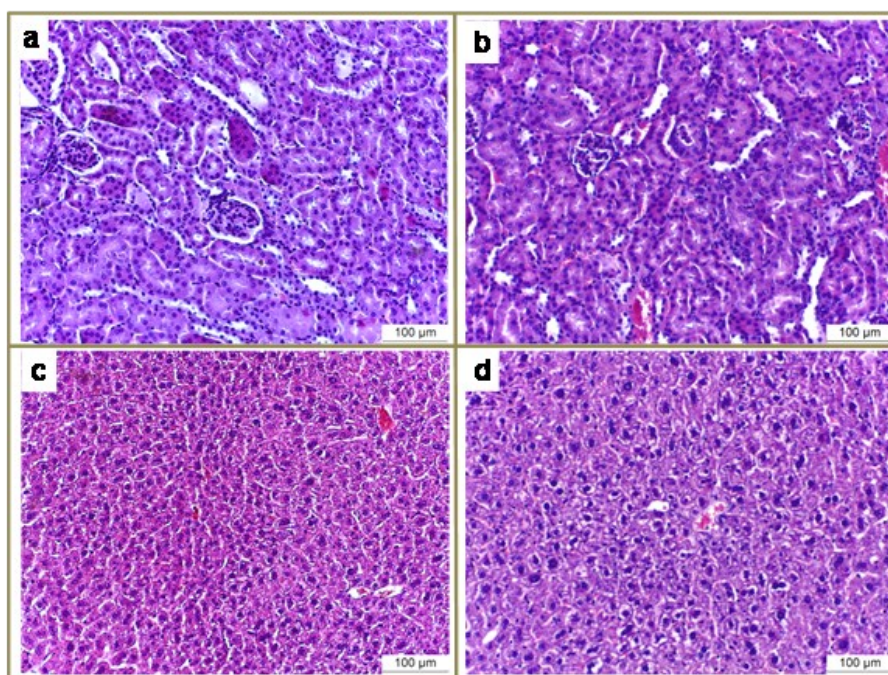


Figure S8. Representative histological sections of renal medulla. A) Renal medulla of control mice. B) Renal medulla of mice injected with ternary nanoparticles, extracted one week after the intravenous injection.

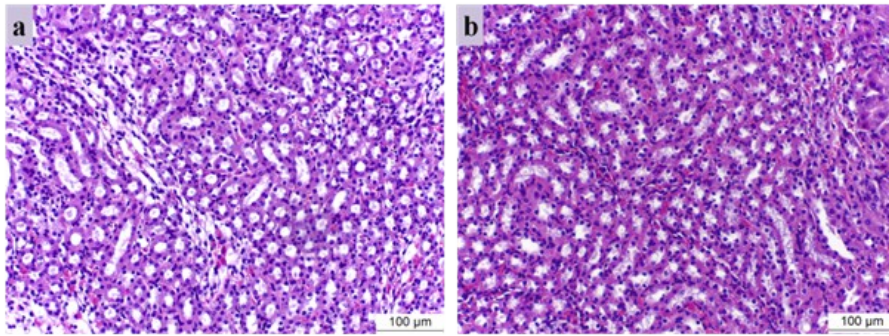


Figure S9. Representative histological sections of spleen. A) Spleen of control mice. B) Spleen of mice injected with ternary nanoparticles, extracted one week after the intravenous injection.

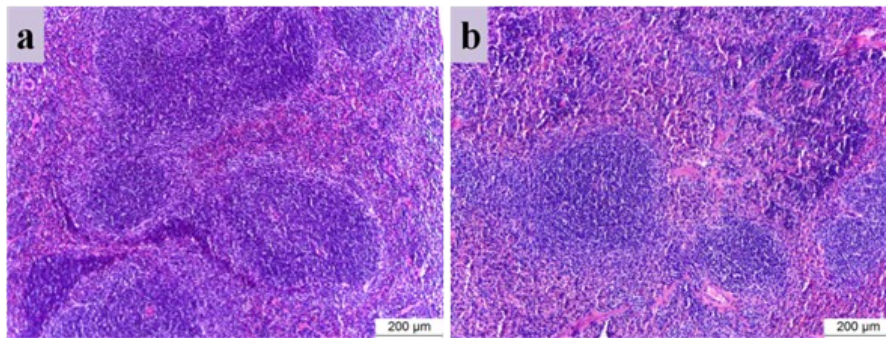


Figure S10. Representative histological sections of spleen. A) Spleen of control mice. B) Spleen of mice injected with ternary nanoparticles, extracted one week after the intravenous injection.

b) Weight control:

Animals injected with ternary NPs showed a small decrease of weight in the first 24 h, very likely due to the stress cause by the experimental procedure and to the anesthesia. This slight decrease in weight was recovered at 48 h post-injection, and from this point the weight profile was similar for both control and injected mice.

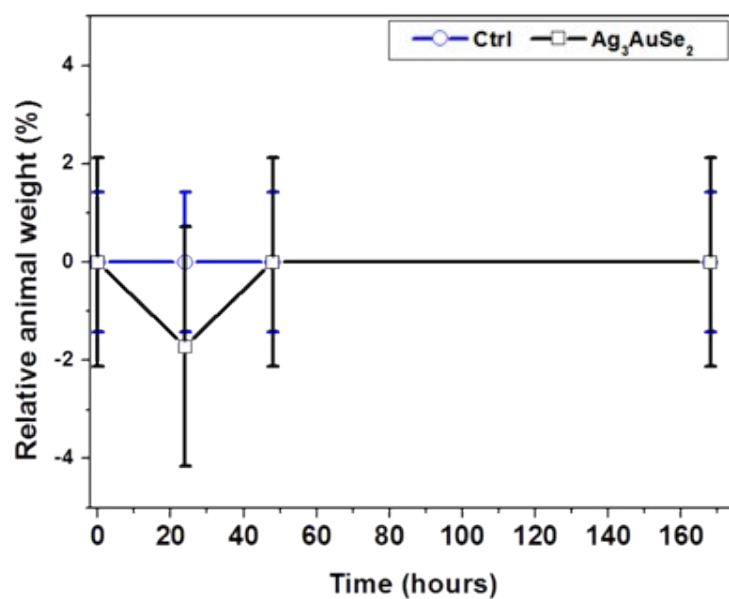


Figure S11. Weight profile of intravenously injected mice and control mice in relative weight.

REFERENCES:

1. C. Caro, M. J. Sayagues, V. Franco, A. Conde, P. Zaderenko and F. Gámez, *Sensors and Actuators, B: Chemical*, 2016, **228**, 124-133.